Available online at www.sciencedirect.com
ScienceDirect
Control Engineering Practice 15 (2007) 277–289
CONTROL ENGINEERING PRACTICE
www.elsevier.com/locate/conengprac

Mechatronics in fuel cell systems

Anna G. Stefanopoulou*, Kyung-Won Suh

Mechanical Engineering Department, University of Michigan, 1231 Beal Avenue, Ann Arbor, MI 48109, USA

Received 24 March 2005; accepted 8 December 2005
Available online 31 January 2006

Abstract

Power generation from fuel cells (FCs) requires the integration of chemical, fluid, mechanical, thermal, electrical, and electronic subsystems. This integration presents many challenges and opportunities in the mechatronics field. This paper highlights important design issues and poses problems that require mechatronics solutions. The paper begins by describing the process of designing a toy school bus powered by hydrogen for an undergraduate student project. The project was an effective and rewarding educational activity that revealed complex systems issues associated with FC technology.

Keywords: Fuel cell; Power; Multivariable; Feedback control; Mechatronics

1. Introduction

The fuel cell (FC) principle dates back to the early 1800s (Schœnbein, 1839). Only recently, however, have FCs become a promising alternative to internal combustion engines (ICEs) and thus are considered for transportation (automotive, marine and aerospace) applications and distributed power generation. FCs are very efficient because they rely on electrochemistry rather than combustion. Specifically, water, electrical energy, and heat are created through the combination of hydrogen and oxygen. The major breakthroughs that have recently brought FCs to the fore-front include the development of low resistance membranes, highly diffusive electrodes, and reduced use of noble metal catalysts. Moreover, efficient power electronics and electric motors can now effectively utilize and distribute the electricity generated from the FC. All these advances have led to many experimental demonstrations. It is the application of mechatronics concepts, however, that will allow the FCs to move from laboratories to streets, powering automobiles, or to our basements, heating and cooling our houses.

Our ability to precisely control the reactant flow and pressure, stack temperature, and membrane humidity is critical for the efficiency and robustness of the FC stack system in real world conditions. These critical FC parameters need to be controlled for a wide range of operating conditions by a series of actuators such as relays, valves, pumps, compressor motors, expander vanes, fan motors, humidifiers and condensers. Precise control with low parasitic losses is the challenging goal of the FC auxiliary system. Moreover, estimation and real time diagnostics should be developed to augment the limited sensing capability in FCs. Finally, a snapshot into the FC industrial arena, namely, partnerships and joint ventures among automotive companies, component suppliers, and development laboratories indicates that there is a strong need for modular control architectures. FC vehicles, for example, have an FC stack controller, vehicle (e.g. chassis, cooling) controllers, and an electric traction motor (TM) controller. Guidelines for the hierarchy and the coordination of all these controllers will allow their independent development and ensure a minimum level of integration.

The interactions among many thermal, chemical, electrical, and psychrometric subsystems require complicated models that are neither easy to compile nor simple to use in model-based controllers. This paper presents various FC subsystems, their models, and their integration from a controls and mechatronics perspective. The paper starts with a containable FC design project that was undertaken within one semester by a team of undergraduate students.

*Corresponding author. Tel.: +1 734 615 8461; fax: +1 734 764 4256.
E-mail address: annastef@umich.edu (A.G. Stefanopoulou).

0967-0661/$ - see front matter © 2006 Elsevier Ltd. All rights reserved.
doi:10.1016/j.conengprac.2005.12.003

The FC design is described in detail to familiarize the reader with the FC dimensions and parameter values. Despite the simplicity of the design project, it presents a concrete case study where design and control iterations are needed. The sections that follow the design project provide a comprehensive discussion of the FC system.

2. The FC toy school bus

A team[1] of four senior undergraduate students in the Mechanical Engineering Department at the University of Michigan designed and built a toy hydrogen powered bus that runs at constant speed around a hilly route emitting only water. The road grades were modeled after a popular university bus route, which is currently served every 15 min by buses powered with diesel fuel or natural gas. The semester-long project allowed us to understand the mechatronics and design issues surrounding hydrogen-powered vehicles. The project and its pedagogical aspects stressed cross-disciplinary involvement and combined control and design concepts for the analysis and synthesis of technologies important to our environment. Fig. 1 shows three of the team members on the day the project was exhibited to the public and the jurors.

Fig. 1. Tim, Sarah, and Dave (from left) putting the final touches to their FC toy bus.

2.1. The FC toy bus propulsion

The design goals included a small size (less than $20 \times 12 \times 8\,\text{cm}^3$) and light weight toy bus that can run for 3 h on 15% road grades at 10 cm/s velocity. The total project budget was less than $1500. The selection and sizing of the toy FC bus components was challenging because there were few benchmark examples that could provide initial data. Moreover, linear scaling did not apply to the power, volume, and weight of FC vehicles so published data from experimental full-size FC vehicles could not be used. A further challenge was that commercially available FC components in the desired range of size and weight considerably narrowed the design parameter space.

A FC stack of three (3) proton exchange membrane (PEM) cells with maximum power 3 W was found in a FC store (Fuel Cell Store, n.d.). It was fortunate that a FC at this lower power range was available, but it was quickly realized that the FC toy bus would have a very low specific power when compared to full size experimental FC vehicles which have reached 200 W/kg (Friedlmeier, Friedrich, & Panik, 2001). The 3 W FC stack weighed 1 kg with dimensions $89 \times 89 \times 51\,\text{mm}^3$. Therefore, the FC stack occupied a fifth of the total bus volume. Moreover, a quick calculation showed that the FC stack weight alone would be 25% of the total weight that the fuel cell could drive uphill at a 15% grade at 10 cm/s speed assuming 20% powertrain efficiency (3 W $\approx$ 4 9.81 0.15 0.1/0.2 kg m/s^2 m/s).

More technical details were obtained from the FC manufacturer. The nominal FC stack voltage V_{st} was specified as 2.4 V at 1 A of current. The FC stack relied on convection for air (oxygen) feed and cooling without the need for a blower. A low pressure hydrogen feed with minimum supply of 2.2 l/h of hydrogen was required. The specified supply corresponded to hydrogen excess ratio $\lambda_{H_2} = (H_2\,\text{supplied})/(H_2\,\text{reacted}) = 1.61$ based on the H_2 reacted to support 1 A of current. Specifically, electrochemistry principles were used to calculate the rate of hydrogen consumption in the FC reaction based on the stack current $I = 1\,\text{A}$, the number of cells $n = 3$, the hydrogen molar mass $M_{H_2} = 2.02\,\text{g/mole}$, the hydrogen density $\rho_{H_2} = 0.0827\,\text{g/l}$ at 20 °C and 100 kPa, and the Faraday number $F = 96485$

$$H_2\ \text{reacted} = \frac{nI}{2F}\frac{M_{H_2}}{\rho_{H_2}}3600 = 1.37\,\text{l/h}. \quad (1)$$

The next step was the identification and sizing of the on-board hydrogen storage. As was the case with the FC selection, the commercially available hydrogen storage options were very limited for the desired power and volume range. A metal hydride storage bottle was found in a FC store. Metal hydride tanks were chosen as alternatives to the liquefied cryogenic or compressed hydrogen storage. Metal hydride absorbs hydrogen and releases heat as the

[1]The team members are alphabetically Timothy D. Klaty, David S. Nay, Jean-Paul Pilette, and Sarah M. Yageman. The project sponsors and advisors are Huei Peng and Anna G. Stefanopoulou. The instructor of the capstone design course ME495 that formalized and evaluated the project is Steven J. Skerlos.

tank is filled with hydrogen. Conversely, the hydrogen is released by reducing the pressure and generating heat (Jeong & Oh, 2002).

The metal hydride bottle was specified as absorbing and releasing 20 l of hydrogen in a volume of 0.74 l and weighed 366 g. The bottle could provide nine continuous hours of run time, based on a supply rate of 2.2 l/h required by the 3 W FC. The manufacturer suggested operating the FC stack without restricting the anode exit and thus maximizing the supply rate. This mode of operation is also known as "open-ended anode". The actual running time that was finally achieved by the FC toy bus was 3.6 times lower than expected, indicating high hydrogen losses or lower stored H_2 volume.

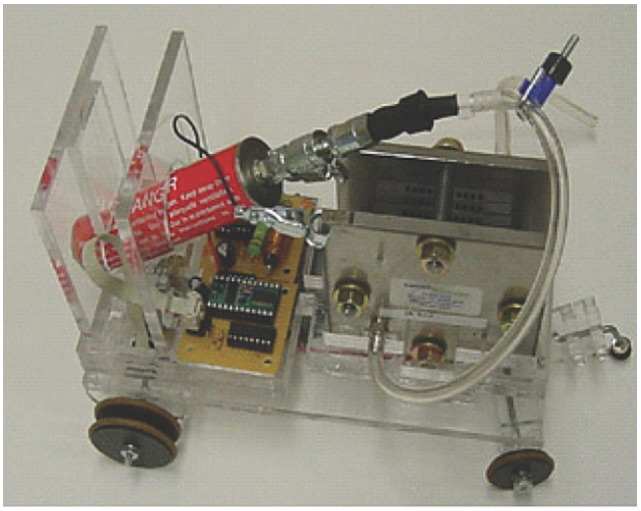

Fig. 2. The components arranged in their final position in the chassis.

The chassis was designed and laser cut out of 0.25″ thick plexiglass. Several layers were stacked and fused with methylene chloride solvent to support the weight of the FC and electronics and prevent excessive bending. The FC stack was placed in the front of the vehicle to allow unobstructed air flow. To accommodate the rear-wheel drive and achieve a good weight balance the electric drive and the hydrogen tank was placed with all the electronics in the rear, as shown in Fig. 2. Two supports were manufactured so that the bottle could slide in and out easily for refilling. Finally, the roof of the bus could be removed to allow for easy access to the components.

The track was designed as a figure-eight manufactured of plywood and plaster. The middle of the track was grooved to guide the front steering mechanism of the bus, which was a simple hinge attached to the front pivoting axle of the toy bus.

2.2. The electric powertrain

Having specified the FC power (voltage and current) and ensuring adequate hydrogen supply the powertrain was designed as follows. The 2.4 V and 1 A was sent to the DC/DC converter where it is stepped up to the output voltage required for the TM. A schematic of the overall powertrain is shown in Fig. 3.

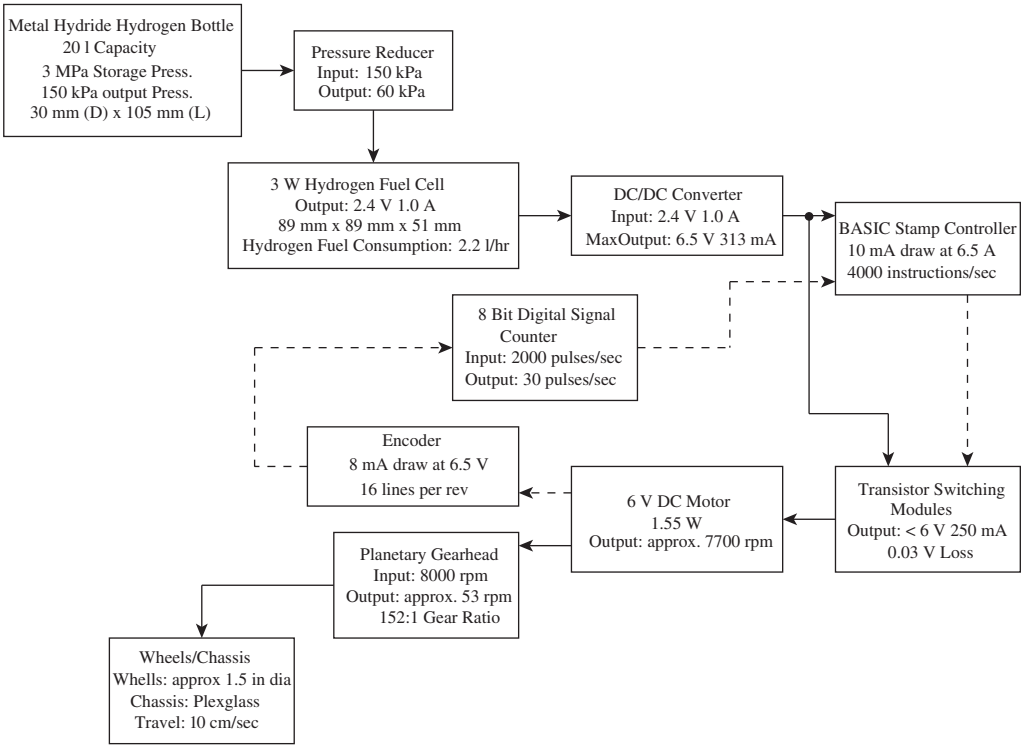

Fig. 3. The information (dashed line) or energy (solid line) flow for the powertrain components along with specifications.

In selecting a motor, several requirements had to be met. These included the power necessary to drive the toy bus, as well as low power consumption, integrated encoder feedback, and a small size. The power requirements were satisfied by the Micromo 1524SR DC motor with an integrated 16 line magnetic encoder. The motor achieves a range of 1.73 W maximum power output with 0.45% efficiency (requires 3.84 W of input power) or 0.76 W output power with the maximum efficiency 0.76% (requires 1.0 W of input power). The DC motor operates at an input voltage range of 5–6.5 V with the optimum being equal to 6 V.

Anticipating some voltage drop from the FC, a DC/DC converter was chosen to step-up the quoted FC stack voltage 2.4–6.5 V in the DC/DC output. The DC/DC converter was implemented using a LM2578A switching regulator manufactured by National Semiconductor. The output of the DC/DC converter was sent to a BASIC stamp controller and a transistor-switching module for current control to the DC motor. The BASIC stamp controller drew $I_{cntr} = 8\,\text{mA}$ at 6.5 V, and output 4000 instructions per second. The encoder, drawing $I_{encd} = 8\,\text{mA}$, measured the angular velocity of the motor and provided the information to the BASIC stamp controller. The inputs to the transistor-switching module were the DC/DC converter power output and the output of the BASIC stamp controller. The heart of this switching module was a TO-92 type transistor made by Zetex that drew $I_{trns} = 40\,\text{mA}$.

The motor drew the current from the transistor-switching module, and used it to mechanically rotate the shaft at a speed that depends on the current delivered. The maximum current that was delivered to the motor was

$$\begin{aligned} I_{m,in} &= I_{dc,out} - I_{loss} \\ &= \eta_{dc} P_{fc} / V_{dc,out} - (I_{cntr} + I_{trns} + I_{encd}) \\ &= 0.85(2.4/6.5) - 0.008 - 0.008 - 0.04 \\ &= 0.258\,\text{A}. \end{aligned} \quad (2)$$

The transistor-switching module then regulated its electrical output and consequently controlled the motor speed up to a maximum of 6 V and 250 mA for the bus to go uphill. A current of 0.250 A corresponds to motor output of 1.113 W with 71.6% efficiency and 7700 rpm based on the manufacturer map. A 152:1 planetary gear results in an axle rotation speed of 53 rpm. The axle's rotational speed was then geared up with 3.8 cm diameter wheels, giving the toy bus a speed of 10 cm/s around the track.

The BASIC stamp controller processed the measured rotational speed of the motor by counting the encoder pulses within 4 ms. The controller then sent a high or low voltage signal to the transistor that in turn controlled the current to the motor. A 2 kΩ resistor was sized and used to match the high–low voltage from the BASIC stamp controller to the on–off voltage inputs to the transistor.

Since the motor was, in effect, turning on and off very rapidly, some safeguards to protect both the motor and the electronics were necessary. Due to the motor's inherent inertia, when no voltage was being applied, the motor continued to spin, forcing current through the line. This could have easily shorted out the transistor if not accounted for. To protect against this, a fly-back diode was placed in parallel with the motor as a safety valve. Also, to eliminate voltage spikes due to the transistor switching a small capacitor (100 pF) was added in parallel.

In summary, the toy FC bus had the following sub-systems shown in Fig. 3: metal hydride storage bottle, 3 W fuel cell, DC/DC converter, BASIC stamp controller, transistor-switching module, 6 V DC motor, digital encoder, planetary geartrain, wheels/chassis, steering, and track.

2.3. Hybrid FC+battery power

After frantic preparation and multiple inspections of the individual components the students connected all the parts except the H_2 supply. The toy bus and its track were taken to a space with adequate ventilation in case of a potential H_2 leak. The fully charged metal hydride tank was connected to the FC anode inlet and FC toy bus started spinning its wheels.

In its initial run, the toy bus ran through the flat part of the track but was unable to negotiate the 15% grade. Further investigation showed us that the FC voltage dropped to 1.8 V at 1 A current which prevented the FC toy bus from being pulled up the specified grade. In hindsight the low voltage (0.6 V per cell) was more realistic given other published data, so it was not possible to complain to the manufacturer except to ask for a FC with larger active area that would allow higher current at 0.6 V per cell, or the integration of one more cell into the stack. Requesting a new FC stack was not, however, an option because a new FC volume and weight would require substantial re-design.

Power augmentation with batteries was an obvious design option and offered an easy solution to the problem. Indeed, when three AA batteries were added in parallel to the output of the DC/DC converter, the FC-hybrid toy bus could climb the track slopes. The three batteries added no significant weight and they could fit under the hydrogen tank without modifications. The operation of DC/DC converter changed to current controlling mode with floating battery voltage.

The electric and power flow configuration of full size hybrid FC vehicles is very similar to our approach especially when a high voltage battery is sized and connected in parallel to the load that (i) maintains constant electric-bus voltage despite FC stack voltage variations, (ii) acts as a load buffer to the FC stack. Different hybrid configurations are described with their benefits and drawbacks in Section 3.4.

Table 1
Fuel cell toy bus performance

Performance measures	FC toy bus	NECAR4
Power density (W/m^2)	300	5000
Specific power (W/kg)	3	200
Efficiency (tank-to-wheel in mi/gal of gasoline)	3.75	60

2.4. Results and lessons learned

The bus was able to operate for 2.5 continuous hours on the specified track starting with a full hydrogen tank. The batteries remain 80% full after the 2.5 h run. Note here that the batteries alone could not make the wheels spin on a flat terrain indicating that the FC was supplying most of the traction power.

Despite the overall project success, neither the FC stack nor the metal hydride tank met their original design specifications. Based on the 20 l (1.6 g) of H_2 stored in the metal hydride tank and the 1 km of distance traveled (10 cm/s for 2.5 h), the calculated fuel consumption of the FC toy bus was equivalent to 1.6 km/l (3.75 mi/gal) of gasoline fuel. In comparison, the NECAR 4 FC experimental full size vehicle[2] achieves 25 km/l (60 mi/gal) of gasoline fuel as summarized in Table 1.

In an effort to identify the reasons for the low efficiency one has to understand the FC system fundamental parameters, especially, the hydrogen and air flow rates, the membrane humidity, and the stack temperature. First, the FC stack selected relies on convection for its air supply and cooling. Increasing the air flow with a fan might have improved the FC voltage at the expense of increased parasitic power to spin the fan and the additional mass and volume associated with the fan. Second, in our bus there was no humidification of the incoming air, which could have dried the membranes and increased the total cell resistance. External humidification was not possible because it is cumbersome and excessive vapor generation can cause many problems to the FC and the electronics in its proximity. Finally, the hydrogen flow discharged by the metal hydride tank depends on the tank temperature. As the tank releases hydrogen, it becomes cold, which restricts the release of further hydrogen. Considerable vapor condensation of the ambient humidity during the 2.5 h operation was stark evidence of this cooling effect. It therefore would have been reasonable to insulate the tank and integrate an isolated thin heating element to improve the overall system performance.

The FC toy school bus project was done as an exercise in defining and integrating the powertrain components of an electric car. The FC stack was treated as a (heavy rechargeable) battery that provided current at a nominal voltage. Upon completion of the project, it was obvious to all of us that a FC-powered powertrain is more complex and depends on optimization of the whole system instead of individual components.

[2]In March 1999, DaimlerChrysler introduced NECAR 4, a compact fuel-cell-powered car fuelled with liquefied hydrogen (LH_2) with approximately 450 km range (Friedlmeier et al., 2001).

3. Fuel cell operation

As highlighted by the FC toy bus project, FC systems (FCS) require the integration of chemical, fluid, mechanical, thermal, electrical, and electronic subsystems. Understanding the important physical variables and their underlying interactions is indispensable for the system design and the overall performance. This section presents the principles of FC operation with the goal of highlighting the mechatronics and cross-disciplinary aspects of FCSs.

There are different types of FCs (US Department of Energy, Office of Fossil Energy & National Energy Technology Laboratory, 2004) distinguished mainly by the type of electrolyte used in the cells, including polymer electrolyte FC (PEMFC, also known as proton exchange membrane FCs), alkaline FC (AFC), phosphoric acid FC (PAFC), molten carbonate FC (MCFC), and solid oxide FC (SOFC) (Fig. 4). The differences in cell characteristics, cell material, operating temperature and fuel need to be taken into account for different applications. Operating below or near the boiling temperature of water, PEMFCs and AFCs rely on protons or hydroxyl ions as the major charge carriers in the electrolyte, whereas in the high-temperature FCs (MCFC and SOFC) carbonate ions and oxygen ions are the charge carriers. The ability of MCFC and SOFC to operate on carbonate ions and oxygen ions makes them fuel flexible. On the contrary, the PEMFC dependence on high-purity hydrogen reactant requires novel hydrogen generation and storage technologies. PEMFCs have high power density, a solid electrolyte, and long life, as well as low corrosion (Larminie & Dicks, 2003). PEM FCs operate in the temperature range of 50–90 °C which allows fast start-up and shut-down. Due to

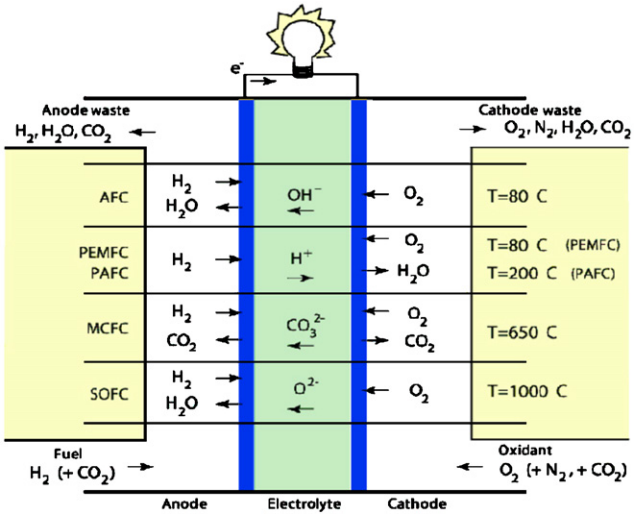

Fig. 4. Fuel cell types.

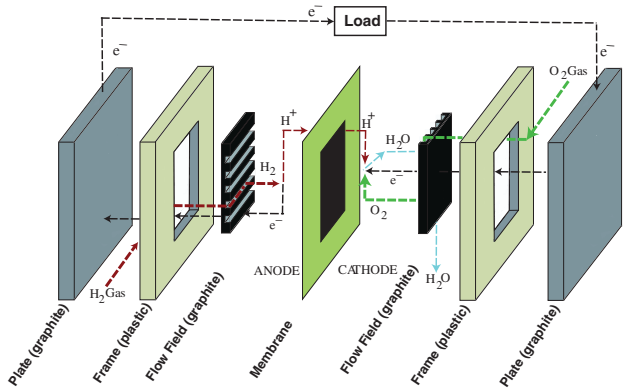

Fig. 5. Fuel cell component description.

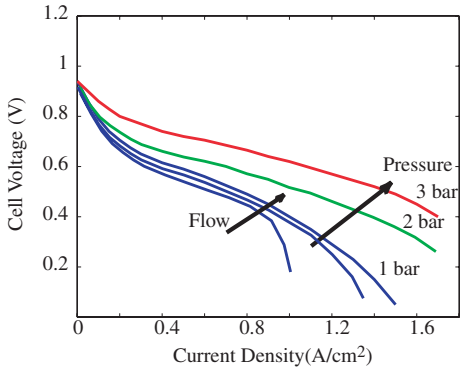

Fig. 6. Polarization curves for different cathode pressures.

their benefits and advanced stage of development, PEMFC was used for the toy bus and is the focus of this paper.

PEMFCs utilize the chemical energy from the reaction of hydrogen and oxygen (referred to as "fuel" from this point on) to produce electricity, water and heat. As shown in Fig. 5, fuel travels through inlet manifolds to the flow fields. From the flow fields, gas diffuses through porous media to the membrane. The membrane, sandwiched in the middle of the cell, typically contains catalyst and micro-porous diffusion layers along with gaskets as a single integrated unit. One side of the membrane is the anode and the other is the cathode. The anode and cathode are more generally described as electrodes. The catalyst layer at the anode separates hydrogen molecules into protons and electrons ($2H_2 \rightarrow 4H^+ + 4e^-$). The membrane permits ion transfer (hydrogen protons), enabling the electrons to flow through an external circuit before recombining with protons and oxygen at the cathode to form water ($O_2 + 4H^+ + 4e^- \rightarrow 2H_2O$). This migration of electrons produces electricity, which is the useful work. The overall reaction of the FC is therefore $2H_2 + O_2 \rightarrow 2H_2O + \text{heat}$.

The electrical characteristics of FCs are normally given in the form of a polarization curve, as shown in Fig. 6, which is a plot of cell voltage versus cell current density (current per unit cell active area) at different reactant pressures and flows. Stack temperature and membrane water content also affect the FC voltage. The difference between the actual voltage and the ideal voltage[3] represents the loss in the cell which turns into heat. As more current is drawn from the FC, the voltage decreases, due to FC electrical resistance, inefficient reactant gas transport, and low reaction rate. Lower voltage indicates lower efficiency of the FC, hence, low load (low current) operation is preferred. However, operation at low load requires a large FC stack, which adversely affects the overall volume, weight, and cost.

Instead of over-sizing the FC stack, a series of actuators such as valves, pumps, blowers, expander vanes, fan motors, humidifiers and condensers shown in Fig. 7 are used to control critical FC parameters for a wide range of current, and thus, power setpoints. The auxiliary actuators are needed to make fine and fast adjustments to satisfy performance, safety and reliability standards that are independent of age and operating conditions (Yang, Bates, Fletcher, & Pow, 1998). The resulting multivariate design and control synthesis task, also known as balance of plant (BOP), is complex because of subsystem interactions, conflicting objectives, and lack of sensors. The main control tasks are summarized next with an emphasis on the interactions and conflicts among the main FC subsystems: (i) reactant supply system, (ii) heating and cooling system, (iii) humidification system, and (iv) power management system.

3.1. Reactant flow management

The reactant flow subsystem is necessary to rapidly replenish the depleted hydrogen and oxygen associated with the current drawn (load) from the anode and cathode. A low partial pressure of oxygen (hydrogen) in the cathode (anode) causes oxygen (hydrogen) starvation that can damage the FC or significantly reduce its life (Yang et al., 1998). The hydrogen and air supply must be coordinated so that the pressure difference across the FC membrane is small enough to prevent membrane damage. To minimize resistive losses, membranes are very thin. The desired air pressure is slightly lower than the hydrogen pressure to avoid air leaks towards the anode which can form combustible mixture. Issues associated with the hydrogen generation or storage are not discussed in this paper. Models, controllers, and references for a natural gas fuel processor can be found in Pukrushpan, Stefanopoulou, and Peng (2004b). Details for hydrogen generation using aqueous borohydride solutions are found in Amendola et al. (2000). Information on hydrogen storage using metal-hydride tanks can be found in Jeong and Oh (2002).

Passive FC systems such as the PEMFC used in the toy bus project, rely on convective flow with low power density. In low cost FC systems a fixed speed (or three speed) motor provides the air supply to satisfy maximum traction requirement. At low flow demand the motor is a

[3]The ideal standard voltage for a FC in which H_2 and O_2 react is 1.18 V when the resulting water product is in gaseous form.

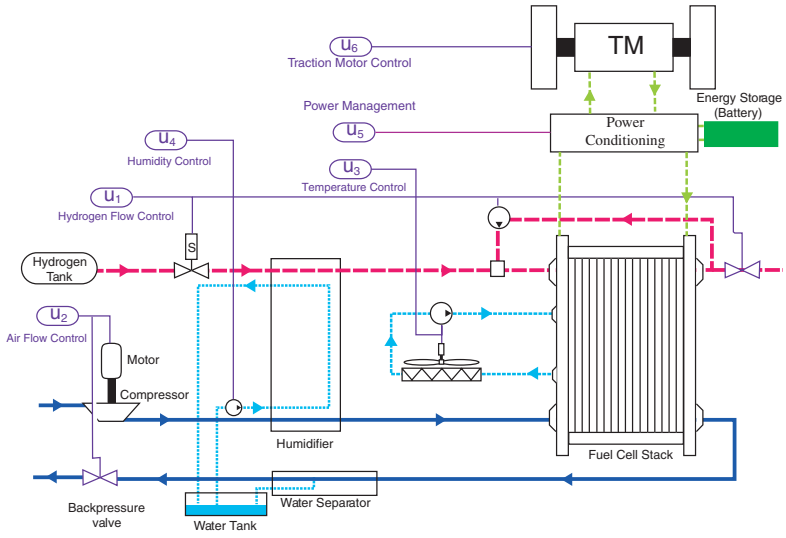

Fig. 7. Fuel cell powertrain system.

mere parasitic loss that decreases the overall propulsion efficiency at low loads, creates start-up problems and, as is discussed next, adversely affects the MEA hydration. To mitigate these problems, a compressor (or a blower) motor control command u_2 can be used to regulate the air flow to the cathode of the FC stack. A pressure regulator u_1, as shown in Fig. 7, can easily control the anode pressure to follow the cathode pressure if compressed hydrogen is available. When reformed hydrogen is supplied by a fuel processor system (FPS), the operating FC pressure is typically close to atmospheric to minimize losses. The cathode flow is then controlled to follow the anode flow or pressure. The responsiveness of the reactant flow system then depends on the hydrogen supply, as discussed in detail in Pukrushpan et al. (2003). The control architecture, control loop tuning, and hierarchy is thus defined in terms of the system operating pressure and the bandwidth of the anode and the cathode supply. Although this approach is reasonable, there are cases where this hierarchy is not so obvious. Multivariable control tools can help analyze the optimum architecture, as presented in Pukrushpan et al. (2003).

Independent of the implications to the control architecture, the cathode operating pressure is an important and free design parameter that has attracted considerable attention, raised heated arguments, and polarized FC developers. Low pressure FC systems rely on a blower, which have both benefits and drawbacks, as follows. Low parasitic losses come unfortunately hand in hand with low FC power density. Inexpensive off-the-shelf blowers meet the air flow specifications, but they are sometimes too bulky. Analysis of the responsiveness for each configuration indicates that the low pressure system can be approximated by a first order system. The response of the low pressure system is limited by the blower inertia, whereas, the high pressure system response is higher order and depends on the supply manifold volume (Gelfi, Stefanopoulou, Pukrushpan, & Peng, 2003). Lastly, blowers do not cause high temperature rise, thus reducing the need for inlet gas cooling before the stack. Low temperature gas, however, cannot carry a lot of humidity which causes the inlet gas humidification and water management to be more sensitive than is the case for high-pressure FC systems that use custom-made compressors. There is no definitive conclusion as to the best pressure system yet, but each system has its champions. Some companies are exploring the flexibility of having a dual pressure system and switching between high and low pressure at different operating loads.

Once the operating pressure has been determined and the control hierarchy has been allocated among actuators and performance variables, feedforward maps (look-up tables) can be derived from the load (current drawn) to the actuators. The immediate question that arises is the availability of sensors for feedback design. Considerations of sensor cost and ruggedness are central to the system configuration. Pressure sensors are cheaper and more rugged so they are preferred over the mass air flow sensors. Other questions arise from the fundamental dependency between flow and pressure (Yang et al., 1998):

- "Should the control problem be posed as one of pressure regulation or one of flow tracking?" in Boettner, Paganelli, Guezennec, Rizzoni, and Moran (2002).
- "Should we control an additional backpressure throttle in the cathode to allow better regulation of both flow and pressure?" in Yang et al. (1998), Pischinger, Schönfelder, Bornscheuer, Kindl, and Wiartalla (2001), Rodatz, Paganelli, and Guzzella (2003).

Recent simulation results in Pukrushpan, Stefanopoulou, and Peng (2004a) indicate that air flow tracking augmented with supply manifold pressure and FC stack (average cell) voltage measurements reduces oxygen

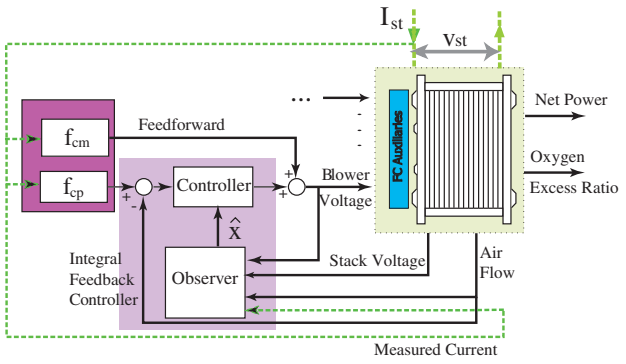

Fig. 8. Potential controller architecture for the air flow management.

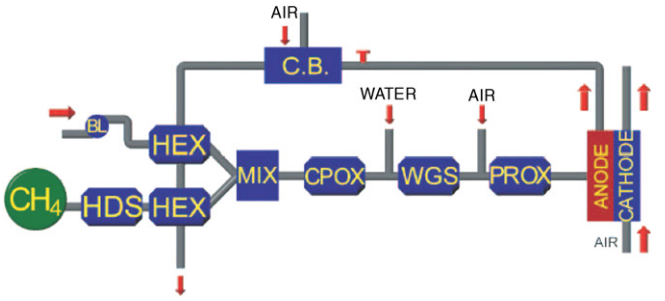

Fig. 9. Schematic diagram of a combined fuel cell and a natural gas fuel processor where heat and power generation are combined for high efficiency.

starvation during load transients. The voltage measurement improves system observability and thus enables a model-based observer and controller design as in the configuration of Fig. 8. Using the stack voltage measurement as a stand-alone virtual starvation sensor might be difficult in practice because voltage depends on other variables such as hydrogen partial pressure (Arcak, Görgün, Pedersen, & Varigonda, 2003), membrane humidification (dryness and flooding) (Görgün, Arcak, & Barbir, 2005; Rodatz et al., 2003), and carbon monoxide poisoning (Rodrigues, Amphlett, Mann, Peppley, & Roberge, 1997). Currently, voltage is used in diagnostic and emergency shut-down procedures due to its fast reaction to oxygen starvation, but its utility and use in a feedback design has not been fully explored.

Efforts have been devoted to controlling the reactant flow system using only voltage and current measurements and inferring power. Specifically, a single-input single-output (SISO) controller between the compressor motor voltage and the delivered current or power to the traction motor TM is cited in Lorenz et al. (1997). As shown in Mufford and Strasky (1999), Pukrushpan et al. (2004a), Suh and Stefanopoulou (2006), when no secondary energy storage elements are included the input–output system (from blower command to FC net power) exhibits an initial inverse response, thus limiting the achievable FC performance.

To prevent stack starvation, the stack current signal is typically filtered by a low-pass filter to allow enough time for the air supply system to increase air flow to the cathode. Since this solution slows down the FC power response, it is desirable to use a current limiter based on a reference governor (Sun & Kolmanovsky, 2004) or a model predictive controller (Vahidi, Stefanopoulou, & Peng, 2004).

3.2. Cooling and heating management

A cooling and heating subsystem is needed to dissipate the heat from the FC reactions and control the temperature of the inlet reactants before they enter the stack. Although the power range and number of cells (only 3 W from three cells) of the FC toy bus did not require active cooling, the heat associated with the range of power needed for a typical passenger vehicle cannot be passively dissipated by convection and radiation through the external surfaces of the FC (Larminie & Dicks, 2003). Consistent low temperature (80 °C) operation, thus, requires active cooling through the reactant air and the water cooling system. An active cooling is achieved by varying the speed of the cooling fan and the recirculation pump in coordination with a by-pass valve. These three control inputs (multi-input system) are not shown as distinct in Fig. 7, but are lumped in one control signal (u_3) for simplicity.

The goal for this control loop is fast warm-up (Boettner et al., 2002), with no overshoot and low auxiliary fan and pump power similar to the cooling system for an ICE (Cortona, Onder, & Guzzella, 2001). However, thermal management in FCs is more challenging than that in ICEs. Specifically, the rule of thumb for the energy balance in ICEs is: 33% for mechanical energy, 33% for energy carried by the exhaust gas, and 33% for energy carried by the cooling system. The associated distribution in FC which is 40/10/50 places stringent requirements in the cooling system. Moreover, the low temperature difference between the FC and the environment limits the heat transfer from the coolant to the ambient air. The typical radiator heat rejection capacity is analogous to the temperature difference between the coolant (80 °C in FCs and 120 °C for ICEs) and the ambient air (32 °C) as discussed in Fronk, Wetter, Masten, and Bosco (2000). Hence to achieve good heat rejection capability, FC vehicles need large radiators.

The complexity of the thermal management problem increases when the PEMFC stack is integrated with a fuel processor for H_2 generation (Colella, 2003). The complexity arises from the internal feedback loops generated from the heat exchangers as shown in Fig. 9. Heat exchangers are used in an effort to recover the energy of the exiting flow by heating the inlet flows. The resulting systems are known as combined heat and power (CHP) systems and exhibit slow dynamics (Tsourapas, Sun, & Stefanopoulou, 2004). CHP systems require combined control and optimization of their components to achieve high efficiency without compromising the overall system responsiveness.

3.3. Water and humidity management

The ability of the membrane to conduct protons is fundamental to the PEMFC operation and is linearly dependent upon its water content (Zawodzinski et al., 1993). On one hand, as membrane water content decreases, ionic conductivity decreases (Springer, Zawodzinski, & Gottesfeld, 1991), resulting in a decreased cell electrical efficiency, observed by a decrease in the cell voltage. This decrease in efficiency causes increased heat production which evaporates more water, in turn lowering membrane water content even more. The interaction between high temperature and low humidity creates a positive feedback loop. On the other hand, excessive water stored in the electrodes obstructs fuel and air flow, resulting in cell flooding (Zawodzinski et al., 1993). Detecting water flooding (Barbir, Wang, & Gorgun, 2005) and managing the water concentration in the electrodes (Karnik & Sun, 2005; Rodatz, Tsukada, Mladek, & Guzzella, 2002) is very important for increasing optimal FC efficiency and extending the PEMFC life.

A water injection or an evaporation mechanism, shown with the command u_4, is used to control the humidity of the reactants and eventually the membrane hydration. Although passive (internal) humidification concepts have been rigorously investigated (Bernardi, 1990; Watanabe, Uchida, Seki, Emori, & Stonehart, 1996), external active control allows wider range of operation typically met in automotive applications (Yang et al., 1998).

To design an active humidification system for PEMFCs, a model of the water transport through the membrane is required. The model can be used to predict the anode and cathode humidity level because humidity sensors are currently expensive and cumbersome to install. As current is drawn from the FC, water is generated in the cathode and water molecules are dragged from the anode to the cathode. This transfer of vapor is known as electroosmotic drag. Additionally, the vapor concentration gradient causes diffusion of water through the membrane, in a process known as back diffusion. The magnitude and direction of the net vapor flow through the membrane (anode to cathode or cathode to anode) is a function of the relative magnitudes of these two transport mechanisms.

Perturbation in the FC humidity can be caused by different mechanisms as characterized in McKay and Stefanopoulou (2004): (i) the water generated during the load increase (current drawn from the FC), (ii) changes in absolute and relative reactant pressure across the membrane, (iii) changes in the air flow out of the FC that carries vapor and dries the membrane, and (iv) changes in the FC temperature, and thus, evaporation or condensation. These mechanisms indicate strong and nonlinear interactions among the humidity control task, the reactant flow management loop, the heat management loop and the power management loop. The interactions are so strong that part of the hydrogen flow subsystem is dedicated to water management in the anode. The anode is particularly vulnerable to flooding since it is dead-ended, making it prone to vapor and inert gas accumulation. Various ingenious mechatronic solutions have been proposed to abate anode flooding (Rodatz et al., 2002). The aim of these investigations is to optimize the inefficient practice of purging or recirculating the anode contents utilizing a downstream anode valve and a pump, as shown in Fig. 7.

Pointing to the complexity of the humidification task Büchi and Srinivasan (1997) note that the humidification components account for 20% of stack volume and weight. The stack, on the other hand, under-performs with 20–40% lower voltage if humidification control is inadequate.

3.4. Power management

The simplest power configuration consists of an FC, a DC/DC converter, and a TM (DC motor or inverter and AC motor). The DC/DC converter can make the FC voltage output compatible with the input to the inverter or the DC motor (Larminie & Dicks, 2003; US Department of Energy, Office of Fossil Energy & National Energy Technology Laboratory, 2004; Wang et al., 1998). The DC/DC converter switching frequency, capacitor, and inductor are sized so that the converter produces acceptable ripples in the output voltage and FC current. Due to the low-voltage/high-current output characteristics, the overall switching and nonlinear FC + DC/DC system is very sensitive to load variations (Appleby & Foulkes, 1989). Typically, the traction motor is viewed as a load from the FC + DC/DC side. In the worst case scenario, the load can be modeled as an instantaneous resistive load (R in Fig. 10). The DC/DC converter must then maintain constant output voltage V_{out} (electric bus) during fast load change.

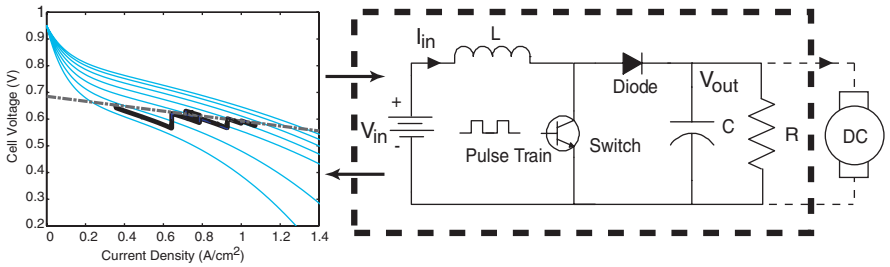

Fig. 10. Simplified electric circuit for a FC connected to a traction motor through a DC/DC converter.

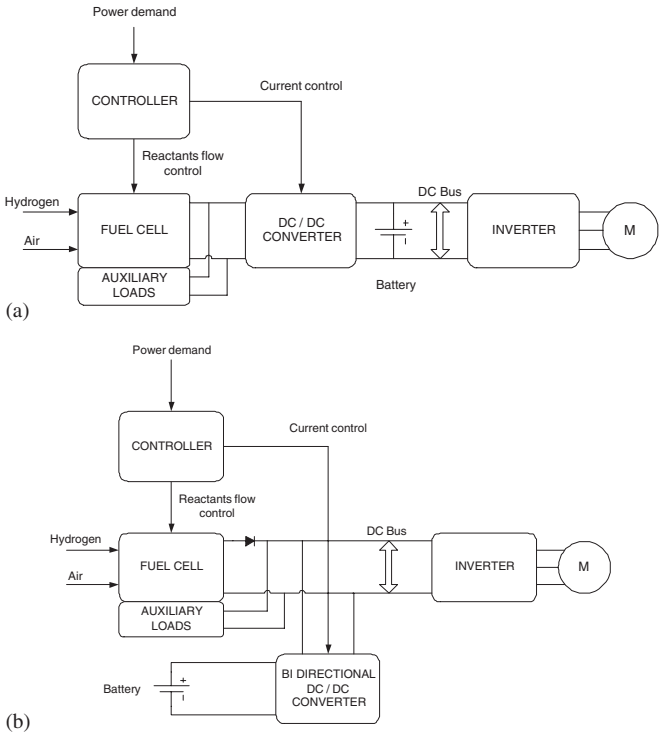

Fig. 11. Electric configurations for fuel cell hybrid vehicle. (a) FC+DC/DC converter with a high voltage battery. (b) FC directly connected to the load with bi-directional converter+battery.

Voltage regulation can be achieved by adjusting the duty ratio of the DC/DC converter pulsewidth (u_5 in Fig. 7). The FC stack can be modeled with its equivalent impedance Z_{FCS}. Note here that it is necessary to consider the closed loop FC system impedance, i.e., calculate the FC impedance once the air flow, the thermal, and the humidification controllers are designed (Pukrushpan et al., 2004a). Coordination of air flow control and DC/DC control alleviates the conflict between supporting proper voltage or power to the bus and preventing stack starvation during fast load change (Suh & Stefanopoulou, 2005).

Hybrid power management studies have included secondary large batteries (Akella, Sivashankar, & Gopalswamy, 2001; Boettner, Paganelli, Guezennec, Rizzoni, & Moran, 2001) and/or ultracapacitors (Rodatz, Paganelli, Sciarretta, & Guzzella, 2005). Several electrical configurations have been considered for hybrid (FC and battery) systems. An excellent discussion for these issues is given in US Department of Energy, Office of Fossil Energy and National Energy Technology Laboratory (2004), Rajashekara and Martin (1995). Fig. 11(a) shows a typical load-leveling or load-sharing FC hybrid configuration that extends FC power using the high voltage battery. The DC/DC converter boosts the stack voltage of the FC to the battery voltage and draws the current from the stack. The battery current supplements the FC current in order to satisfy the power demand. During regenerative braking the DC/DC converter switches off and charge is stored in the battery. In Fig. 11(b), the major power flows from the FC to the load directly without a DC/DC converter. Here a small amount of battery current flows through the DC/DC. This configuration can be more efficient than configuration (a) because it avoids the DC/DC converter losses, however, it relies on the ability of the FC to follow the load demands. The controller that splits load to the FC and battery can be achieved indirectly by adjusting bus voltage using battery + DC/DC (Ramaswamy, Moore, Cunningham, & Hauer, 2004).

The DC/DC converter control problem becomes simplified when a high voltage battery is connected in parallel between the DC/DC converter and the load. The battery supports the main electric-bus voltage, and the duty ratio of the DC/DC converter controls the current drawn from the FC. Non-causal (also known as "backwards-looking") optimization methods can then be used to evaluate energy storage, acceleration and regenerative braking strategies.

4. Time constants

FCs have been considered for many different applications with an emphasis on commercial power generation and automotive applications. The challenges in automotive applications arise partly due to the low cost requirements and partly due to their high bandwidth requirements. Drivers, for example, are perceptive to lags longer than 0.2 s during acceleration requests. The relevant time constants for an automotive propulsion-sized PEMFC stack system are:

- electrochemistry $O(10^{-19})$ s,
- hydrogen and air manifolds $O(10^{-1})$ s,
- vapor dynamics in the cathode $O(10^{0})$ s and in the anode $O(10^{1})$ s,
- flow control/supercharging devices $O(10^{0})$ s,
- vehicle inertia dynamics $O(10^{1})$ s,
- cell and stack temperature $O(10^{2})$ s,

where O denotes the order of magnitude. The fast transient phenomena of electrochemical reactions have minimal effects in automobile performance and can be ignored. The relatively slow dynamics of the vehicle inertia and the cell and stack temperature may be lumped in a separate system which is equipped with a separate controller. The vehicle velocity and stack temperature can then be considered as constant or slow varying parameter for other faster subsystems. The dynamical behavior of water (in vapor and liquid state) in FC depend on many complex mechanisms such as condensation, evaporation, capillary flow and diffusion dynamics. It is thus difficult to establish a time constant for the water dynamics. For example, the time constant for water diffusion in the membrane is smaller than the time constant for the flow dynamics (Wang & Wang, 2005). However, the diffusion mechanism alone does not define the overall water dynamics. A linearization of the gas humidity (vapor water) model in McKay and Stefanopoulou (2004) revealed that the

eigenvalues associated with the cathode and the anode humidity depend on the cathode and anode outlet gas flow, respectively. This finding substantiates the general belief that the humidity dynamics cannot be easily decoupled from the temperature and flow dynamics. Indeed, the air exiting the stack carries considerable vapor and affects the FC humidification. Moreover, the air flow dynamics correspond to time constants that are easily perceived by the driver. Hence, the air flow dynamics described by the manifold filling and supercharging devices need to be considered carefully in the control system design.

5. Experimental set-up

One of the most challenging characteristics in FC technology is its spatially varying behavior which depends on the local temperature and the gas composition at the membrane surface. Due to the complexity inherent in distributed parameter analysis, the geometric complexity of the stack design, as well as the difficulty associated with taking measurements at the membrane surface or within the electrodes of large multi-cell stacks (Mench, Dong, & Wang, 2003), lumped parameter models are used. These lumped parameter models are calibrated using stack measurements. Unfortunately, experimental data necessary for understanding, predicting, and controlling the unique transient behavior of PEMFC stacks are not easy to obtain. It is not easy for example to obtain data from industry or laboratories due to the confidential and competitive nature of the information. Also commercial FC units are typically bundled with closed architecture controllers that obstruct system identification techniques.

To address the need for data and experimental validation of models and controllers a laboratory was established with partial funding from the National Science Foundation (CMS-0219623). A 24-cell, 300 cm^2, 1.4 kW PEMFC stack was purchased from the Schatz Energy Research Center (SERC) at Humboldt State University and installed at the Fuel Cell Control Laboratory (FCCL) at the University of Michigan. Fig. 12(a) displays the instrumented stack installed on the test station at the University of Michigan's Fuel Cell Control Laboratory. Protruding from the stack endplates are the relative humidity, temperature and pressure transducers as well as gas and coolant connections. Fig. 12(b) provides a schematic describing the location of the manifolds in relation to the membrane surface. Reactant gas (hydrogen or air) flows from the inlet manifolds to the flow fields. From the flow fields, gas diffuses through the gas diffusion layers to the active area (catalyst coated area of the membrane). The arrows show the flow of hydrogen and air into and out of the stack. The instruments that monitor relative humidity, pressure, mass flow and temperature are listed in Table 2. The sensor specifications were provided by the manufacturers and have not been independently verified.

The FC operates on a test station with integrated controls, diagnostics, and safety mechanisms. The air control system regulates the air flow at a desired stoichiometric level (200–400%) or at a fixed air flow value. The MKS air flow controller handles dry air supplied by an Atlas-Copco SF1-4 stationary oil-free air scroll-type compressor though an integrated dryer and pressure-controlled ballast tank. The fuel is stored in high-pressure, high-purity hydrogen cylinders. The hydrogen control system reduces the pressure to a level appropriate for delivery to the FC stack and then regulates the anode pressure to a desired level, which is typically set higher than the cathode pressure. Deionized water is used as a medium to either heat or cool the stack in the test station using electric resistance heating and a heat exchanger with a controllable (on–off) fan. The thermostatic controller accepts a set-point and upper–lower thresholds for the power section outlet temperature of the coolant. An electric pump recirculates the coolant through a reservoir that is refilled. The coolant flow rate is controlled through a manual valve.

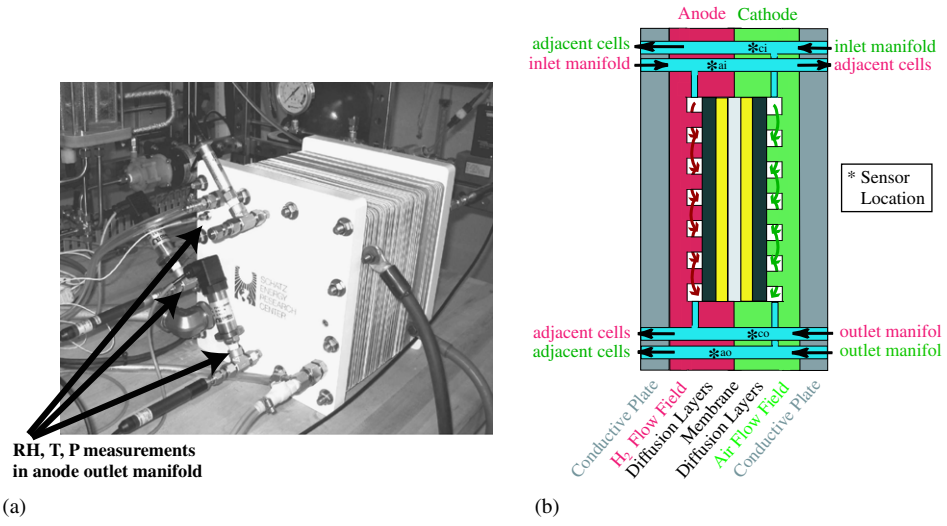

Fig. 12. Instrumented SERC fuel cell stack. (a) Fuel cell stack. (b) Locations of sensors.

Table 2
Sensor specifications

Description	Part number	Vendor	Range and accuracy	Response	Location
Air mass flow controller	Type 1559A	MKS	20–200 ± 2 (slm) 0.41–4.1 ± 0.041 (g/s)	500 ms	Upstream of cathode
Hydrogen mass flow meter	HFM201	Hastings	0–100±1 (slm) 0–0.14±0.0014 (g/s)	2 s	Upstream of anode
RH sensor	SPO5 probe (C94 capacitive sensor), M2 series transducer and Pt RTD	Rotronic	0–100% ± 1.5% RH non-condensing, −40 to 85 °C ± 0.3 °C		Anode outlet, cathode inlet and outlet
Pressure transducer	PX4202-005G5V	Omega	0–5 ± 0.012 (psig) 0–34.47 ± 0.083 (kPa)	10 ms	Cathode and anode outlet
Pressure transducer	PX603	Omega	0–30 ± 0.12 (psig) 0–206.8 ± 0.83 (kPa)	5 ms	Anode inlet
RTD	PR-11-2-100-1/16-6-E	Omega	0–100 °C[a]	[a]	Anode inlet

[a]Accuracy and response time limited by DAQ system.

The experimental set-up allows the design, testing, and integration of real-time software for simulation, optimization, control, and diagnostics in transient load conditions. The laboratory is equipped with hardware/software safety system and data acquisition system based on DAQ boards and signal conditioning backplane.

6. Conclusions

This paper presents the challenges of sizing and controlling fuel cell systems. It also points to recent papers in the FC literature that offer control and mechatronics results. Many publications express the need for a systematic control approach to fuel cell power plans. Because most of these publications are in the Chemistry and Chemical Engineering literature they are not readily available to the control community. The field is fast evolving and while there is considerable excitement, there are also many challenges. These challenges can be addressed with systematic tools such as physics-based models and model-based control design. Finally, fuel cells provide exciting test beds for educational activities, as highlighted by the toy bus project. They require multidisciplinary teams and are very rewarding due to their environmental importance.

Acknowledgments

Financial support by the National Science Foundation under contracts CMS-0201332 and CMS-0219623 and the Automotive Research Center (ARC) at the University of Michigan (UMICH) are gratefully appreciated. Many thanks go to J. Luntz (UMICH) for his help and advice on the power electronics and controller implementation for the FC toy bus and also to H. Peng (UMICH), J. Sun (UMICH), P. Lehman (SERC), C. Chamberlin (SERC), L. Guzzella (ETH), and Y.G. Guezennec (OSU) for all the helpful discussions. The authors also thank the FC toy bus team and lab-mates Amey Karnik, Denise McKay, Jay Pukrushpan, Vera Simms, Vasilis Tsourapas, and Ardalan Vahidi.

References

Akella, S., Sivashankar, N., & Gopalswamy, S. (2001). Model-based systems analysis of a hybrid fuel cell vehicle configuration. In: *IEEE proceedings of the 2001 American control conference* (Vol. 3, pp. 1777–1782). Arlington, VA.

Amendola, S. C., Sharp-Goldman, S. L., Janjua, M. S., Spencer, N. C., Kelly, M. T., Petillo, P. J., et al. (2000). A safe, portable, hydrogen gas generator using aqueous borohydride solution and Ru catalyst. *International Journal of Hydrogen Energy*, *25*(10), 969–975.

Appleby, A. J., & Foulkes, F. R. (1989). *Fuel cell handbook*. New York: Van Nostrand Reinhold.

Arcak, M., Görgün, H., Pedersen, L. M., & Varigonda, S. (2003). An adaptive observer design for fuel cell hydrogen estimation. In: *IEEE proceedings of 2003 American control conference* (Vol. 3, pp. 2037–2042). Denver, CO.

Barbir, F., Wang, X., & Gorgun, H. (2005). Pressure drop on the cathode side of a PEM fuel cell as a diagnostic tool for detection of flooding and drying conditions. In: *ASME proceedings of 2005 international conference on fuel cell science, Engineering and Technology*, Ypsilanti, MI. FUELCELL2005-74037.

Bernardi, D. M. (1990). Water-balance calculations for solid-polymer-electrolyte fuel cells. *Journal of the Electrochemical Society*, *137*(11), 3344–3350.

Boettner, D. D., Paganelli, G., Guezennec, Y. G., Rizzoni, G., & Moran, M. J. (2001). Component power sizing and limits of operation for proton exchange membrane (PEM) fuel cell/battery hybrid automotive applications. In: *Proceedings of 2001 ASME international mechanical engineering congress and exposition* (Vol. 2, pp. 1141–1149).

Boettner, D. D., Paganelli, G., Guezennec, Y. G., Rizzoni, G., & Moran, M. J. (2002). Proton exchange membrane fuel cell system model for automotive vehicle simulation and control. *ASME Journal of Energy Resources Technology*, *124*, 20–27.

Büchi, F. N., & Srinivasan, S. (1997). Operating proton exchange membrane fuel cells without external humidification of the reactant gases. *Journal of the Electrochemical Society*, *144*(8), 2767–2772.

Colella, W. G. (2003). Design considerations for effective control of an afterburner sub-system in a combined heat and power (CHP) fuel cell system (FCS). *Journal of Power Sources*, *118*(1–2), 118–128.

Cortona, E., Onder, C.H., & Guzzella, L. (2001). Model-based temperature control for improved fuel economy of SI-engines. In:

Proceedings of the third IFAC workshop on advances in automotive control (pp. 217–222).

Friedlmeier, G., Friedrich, J., & Panik, F. (2001). Test experiences with the DaimlerChrysler fuel cell electric vehicle NECAR 4. *Fuel Cells*, *1*(2), 92–96.

Fronk, M. H., Wetter, D. J., Masten, D. A., & Bosco, A. (2000). *PEM fuel cell system solutions for transportation*. SAE paper 2000-01-0373.

Fuel Cell Store (n.d.). ⟨http://www.fuelcellstore.com⟩

Gelfi, S., Stefanopoulou, A. G., Pukrushpan, J. T., & Peng, H. (2003). Dynamics of low-pressure and high-pressure fuel cell air supply systems. In: *IEEE proceedings of the 2003 American control conference* (Vol. 3, pp. 2049–2054). Denver, CO.

Görgün, H., Arcak, M., & Barbir, F. (2005). A voltage-based observer design for membrane water content in PEM fuel cells. In: *IEEE proceedings of 2005 American control conference* (Vol. 7, pp. 4796–4801). Portland, OR.

Jeong, K. S., & Oh, B. S. (2002). Fuel economy and life-cycle cost analysis of a fuel cell hybrid vehicle. *Journal of Power Sources*, *105*(1), 58–65.

Karnik, A. Y., & Sun, J. (2005). Modeling and control of an ejector based anode recirculation system for fuel cells. In: *Proceedings of the third international conference on fuel cell science, engineering, and technology*, Ypsilanti, MI. FUELCELL2005-74102.

Larminie, J., & Dicks, A. (2003). *Fuel cell systems explained* (2nd ed.). Chichester and Hoboken, NJ: Wiley.

Lorenz, H., Noreikat, K.-E., Klaiber, T., Fleck, W., Sonntag, J., Hornburg, G., et al. (1997). *Method and device for vehicle fuel cell dynamic power control*. United States Patent 5,646,852.

McKay, D. A., & Stefanopoulou, A. G. (2004). Parameterization and validation of a lumped parameter diffusion model for fuel cell stack membrane humidity estimation. In: *IEEE proceedings of the 2004 American control conference* (Vol. 1, pp. 816–821). Boston, MA.

Mench, M. M., Dong, Q. L., & Wang, C. Y. (2003). In situ water distribution measurements in a polymer electrolyte fuel cell. *Journal of Power Sources*, *124*(1), 90–98.

Mufford, W. E., & Strasky, D. G. (1999). *Power control system for a fuel cell powered vehicle*. United States Patent 5,991,670.

Pischinger, S., Schönfelder, C., Bornscheuer, W., Kindl, H., & Wiartalla, A. (2001). *Integrated air supply and humidification concepts for fuel cell systems*. SAE paper 2001-01-0233.

Pukrushpan, J. T., Stefanopoulou, A. G., & Peng, H. (2004a). Control of fuel cell breathing. *IEEE Control Systems Magazine*, *24*(2), 30–46.

Pukrushpan, J. T., Stefanopoulou, A. G., & Peng, H. (2004b). *Control of fuel cell power systems: Principles, modeling, analysis and feedback design advances in industrial control*. London: Springer, Telos.

Pukrushpan, J. T., Stefanopoulou, A. G., Varigonda, S., Pedersen, L. M., Ghosh, S., & Peng, H. (2003). Control of natural gas catalytic partial oxidation for hydrogen generation in fuel cell applications. In: *IEEE proceedings of 2003 American control conference* (Vol. 3, pp. 2030–2036). Denver, CO.

Rajashekara, K., & Martin, R. (1995). Electric vehicle propulsion systems present and future trends. *Journal of Circuits, Systems and Computers*, *5*(1), 109–129.

Ramaswamy, S., Moore, R., Cunningham, J. M., & Hauer, K.-H. (2004). *A comparison of energy use for a indirect-hydrocarbon hybrid versus an indirect-hydrocarbon load-following fuel cell vehicle*. SAE paper 2004-01-1476.

Rodatz, P., Paganelli, G., & Guzzella, L. (2003). Optimizing air supply control of a PEM fuel cell system. In: *IEEE proceedings of 2003 American control conference* (Vol. 3, pp. 2043–2048). Denver, CO.

Rodatz, P., Paganelli, G., Sciarretta, A., & Guzzella, L. (2005). Optimal power management of an experimental fuel cell/supercapacitor-powered hybrid vehicle. *Control Engineering Practice*, *13*(1), 41–53.

Rodatz, P., Tsukada, A., Mladek, M., & Guzzella, L. (2002). Efficiency improvements by pulsed hydrogen supply in PEM fuel cell systems. In: *Proceedings of the 15th IFAC triennial world congress*.

Rodrigues, A., Amphlett, J. C., Mann, R. F., Peppley, B. A., & Roberge, P. R. (1997). Carbon monoxide poisoning of proton-exchange membrane fuel cells. In: *IEEE proceedings of the intersociety energy conversion engineering conference* (Vol. 2, pp. 768–773). Honolulu, HI.

Schœnbein, C. F. (1839). The voltaic polarization of certain solid and fluid substances. *Philosophical Magazine*, *14*, 43–45.

Springer, T. E., Zawodzinski, T. A., & Gottesfeld, S. (1991). Polymer electrolyte fuel cell model. *Journal of the Electrochemical Society*, *138*(8), 2334–2342.

Suh, K.-W., & Stefanopoulou, A. G. (2005). Coordination of converter and fuel cell controllers. *International Journal of Energy Research*, *29*(12), 1167–1189.

Suh, K.-W., & Stefanopoulou, A. G. (2006). Inherent performance limitations of power-autonomous fuel cell system. In: *IEEE proceedings of 2006 American control conference*, submitted for publication.

Sun, J., & Kolmanovsky, I. (2004). Load governor for fuel cell oxygen starvation protection: A robust nonlinear reference governor approach. In: *IEEE proceedings of 2004 American control conference* (Vol. 1, pp. 828–833). Boston, MA.

Tsourapas, V., Sun, J., & Stefanopoulou, A. G. (2004). Modeling and dynamics of a fuel cell combined heat power system for marine applications. In: *Proceedings of eighth WSEAS international conference on systems*.

U.S. Department of Energy, Office of Fossil Energy and National Energy Technology Laboratory. (2004). Fuel cell handbook (7th ed.). Morgantown, WV: EG&G Technical Services, Inc.

Vahidi, A., Stefanopoulou, A. G., & Peng, H. (2004). Model predictive control for starvation prevention in a hybrid fuel cell system. In: *IEEE proceedings of 2004 American control conference* (Vol. 1, pp. 834–839). Boston, MA.

Wang, K., Lin, C. Y., Zhu, L., Qu, D., Lee, F. C., & Lai, J.-S. (1998). Bi-directional DC to DC converters for fuel cell systems. In: *IEEE power electronics in transportation* (pp. 47–51). Dearborn, MI.

Wang, Y., & Wang, C.-Y. (2005). Transient analysis of polymer electrolyte fuel cells. *Electrochimica Acta*, *50*(6), 1307–1315.

Watanabe, M., Uchida, H., Seki, Y., Emori, M., & Stonehart, P. (1996). Self-humidifying polymer electrolyte membranes for fuel cells. *Journal of the Electrochemical Society*, *143*(12), 3847–3852.

Yang, W.-C., Bates, B., Fletcher, N., & Pow, R. (1998). *Control challenges and methodologies in fuel cell vehicle development*. SAE paper 98C054.

Zawodzinski, T. A., Derouin, C., Radzinski, S., Sherman, R. J., Smith, V. T., Springer, T. E., et al. (1993). Water uptake by and transport through Nafion 117 membranes. *Journal of the Electrochemical Society*, *140*(4), 1041–1047.